Robustness Analysis of Eigenstructure Assignment Controllers on Rigid-Flexible Satellites

Crespo, J.* , Aranda, J.** and Alonso, J.F.***

**Professor at theUPM (Universidad Politécnica de Madrid), Madrid, Spain. javier.crespo@upm.es*

***Professor at the UNED (Universidad Nacional de Educación a Distancia), Madrid, Spain. jaranda@uned.dia.es*

**** Professor at theUPM (Universidad Politécnica de Madrid), Madrid, Spain. josefelix.alonso@upm.es*

[Abstract] Flexible spacecraft with attached solar panels may exhibit undesired vibrations and structural deformations. These types of vehicles show an intrinsic coupling of the elements of the structure. The attitude maneuvers performed by flexible spacecraft may cause non-desired deflections of attached flexible elements. Any attitude and orbit control system generally solves these problems using filters that are designed to attenuate the relative deflections of flexible appendages. In this paper, we propose a method for designing attitude static controllers using an eigenstructure assignment (EA) method. A set of requirements were specified from our understanding of the system modes in an open loop. Exhaustive theoretical and numerical simulations were performed on special cases to verify the controller design procedure. In the design of the controller, we considered all of the aspects that relate to the eigenstructure assignment. The primary objective of this paper is to demonstrate the feasibility of obtaining a high degree of decoupling for some selected modes via the application of an EA method. Finally a robustness analysis is perform to the system together with the designed controller by means of a mu-analysis.

Nomenclature

$\boldsymbol{A}$ = State Matrix

$\boldsymbol{B}$ = Control Matrix

$\boldsymbol{C}$ = Output Matrix

$\boldsymbol{G}$ = Gyroscopic Matrix

$\boldsymbol{I}$ = Identity Matrix

$\boldsymbol{K_m}$ = Stiffness Matrix

$\boldsymbol{K}$ = Gain Controller

$\boldsymbol{M}$ = Mass Matrix

$\boldsymbol{Q_{nc}}$ = Nonconservative generalized forces

q_i = Longitudinal generalized coordinate

r_i = Transversal generalized coordinate

$\boldsymbol{u}$ = Generalized Coordinates Vector

$\vec{\boldsymbol{u}}$ = Control Signal

$\boldsymbol{V}$ = Potential Energy

ω_0 = Spacecraft angular speed

$\vec{\boldsymbol{x}}$ = State Vector

$\vec{\boldsymbol{y}}$ = Output Vector

Λ = Eigenvalues Matrix

λ_{di}= Desired eigenvalues

υ_i = Eigenvectors

ϕ, θ, ψ = Roll, pitch and yaw angles

$\phi_i(\xi)$= Longitudinal shape factor

$\Psi_i(\xi)$= Transversal shape factor

I. Introduction

THE flexibility of a spacecraft is a challenge to researchers and to the designers of attitude control systems. Flexible structures can be problematic because of the combination of various effects, such as the minimal damping of important structures, uncertainty regarding frequencies, and modal coupling. All of these factors can impact controller design, especially in terms of closed-loop stability, robustness with respect to parametric uncertainties and the coupling effects of the entire structure.

The vehicle considered in this paper consists of a rigid body with two cantilevered elastic solar panels that are symmetrically attached to a central reference frame with demanding attitude pointing requirements. In modal analysis and attitude control, it is useful to analyze the motion effects between attitude maneuvers and the deformation of solar panels. In addition, it is important to analyze the influence of the deformation of solar panels on the misalignment of the orientation of a spacecraft. A system modal analysis is based on a representative mathematical model for the real system and allows us to thoroughly understand system performance in terms of natural frequencies, damping and coupling effects.

To perform a comprehensive simulation and obtain acceptable results, the mathematical model of the spacecraft must be as similar as possible to the actual system. A mathematical modeling of this type of system may reveal some interesting features that must be taken into account when considering the bending of solar panels and undesired spacecraft structural vibration. In addition, the mathematical model of the system will consider the natural coupling that exists between the rigid and flexible elements of the spacecraft.

The elastic deformations of the solar panels must be consistent with the mechanical boundaries of the system to allow for acceptable attitude pointing of the spacecraft. Different functions of time and spatial variables are used to model these elastic deformations. The Assumed Mode method introduced in this paper will describe the deformation of the solar panels.

The mathematical modeling of flexible spacecraft or any of their elements has received substantial attention in the literature. In this context, the equations of motion for both flexible spacecraft [1] and flexible multibody systems [2] have been obtained, and the problems associated with active vibrations within flexible spacecraft [3], in addition to precision positioning [4], have been addressed. The coupling effects between both rigid and flexible parts of a spacecraft have been considered in [5]. The effects of damping have been reported in [6]. The effects of flexibility under the assumptions of appropriate control methods have been summarized in [7], and the influence of the attitude of the actuators has been discussed in [8]. Interesting aspects that relate to spacecraft configurations and their implications for attitude coupling have been addressed in [9].

A basic modal analysis will enable us to identify two groups of modes, which are designated herein as orbital modes and deformation modes that relate to the dynamic behavior of the system. The orbital modes involve the angular motions of the spacecraft around a fixed frame. The angular movements are defined by Euler angles and are derived from the difference between the orbital and body frames. The deformation modes correspond to the bending of the solar panels.

The controller design is based on the modal control technique known as Eigenstructure Assignment (EA). The EA method places the eigenvalues and the eigenvectors of a linear system into a closed loop with multiple inputs and multiple outputs for desired positions of the complex plane under the assumption of an existing output or state feedback. The EA method relates controllability, the eigenvalues and the eigenvectors within a closed loop [10] and also addresses the performance of the system using partial state feedback [11] and output feedback methods [12]. The concept of a desired eigenstructure with an additional full state and an output feedback has been proposed in [13].

The EA technique has been widely used in the aerospace field, for example, in the design of controllers for civil aircraft [14]. Robustness concepts as derived via the application of EA have been considered in [15]. In addition, this method has been applied to the robust assignment of flexible aerospace structures [16] and to sophisticated applications, such as in the control of tailless aircraft [17]. Other aerospace applications are concerned with flexibility, such as in the case of a highly flexible aircraft, wherein there is coupling between the roll and yaw angles [18]. In addition, EA control laws have also been applied to spacecraft launchers [19]. Certain aspects of the global methodology of the EA approach [20] have been included in several different toolboxes [21 – 22].

When formulating a controller design based on the EA method, the basic modal data obtained from a previous open loop analysis serves to minimize the elastic vibrations of the solar panels and control the elastic deformations as closely as possible to a quasi static maneuver for a closed loop system.

We considered two special cases to attenuate the deformation of solar panels. First, a general model with a nominal damping in the bending mode was considered. Second, we considered a model that enabled the modification of nominal damping to obtain a prescribed vibration and deflection on solar panels.

II. Problem Formulation

A. Mechanical Model

The equations of motion obtained during the development of the mathematical model must be representative of the actual system, leading to nonlinear kinematics and a dynamics model that can be considered an evaluation model. The evaluation model will be used to validate the controller and to produce numerical results. Three reference frames were taken into account in the development of our mathematical model. The first is the Earth-Centered Inertial (ECI) reference frame. The second is an orbit reference frame, which is located at the center of mass of the satellite ($\mathbf{X_O} - \mathbf{Y_O} - \mathbf{Z_O}$). In this frame, the $\mathbf{Z_O}$-axis points toward the Earth's center, the $\mathbf{X_O}$-axis is tangential to the orbit, and the $\mathbf{Y_O}$–axis is perpendicular to the $\mathbf{X_O}$-axis. The attitude maneuvers are related to rotations around ($\mathbf{X_O} - \mathbf{Y_O} - \mathbf{Z_O}$). They are performed by the spacecraft within the fixed body reference frame ($\mathbf{X_B} - \mathbf{Y_B} - \mathbf{Z_B}$) and are designated as roll, pitch and yaw, respectively. These rotations are identified as orbital modes for the purpose of our controller design strategy. Finally, the body reference frame is located at the center of mass of the satellite and coincides with the principal axis of inertia.

The model of rigid-flexible spacecraft dynamics is based on some general assumptions:

- The flexible appendages (solar panels) are symmetrically attached with respect to the rigid hub. In addition, it is assumed that both appendages are identical.
- The flexible appendages are assumed to be a clamped-free beam in the Y-axis and a free-free beam in the Z-axis.
- The beam is free to undergo vibrations in the longitudinal direction of the Y-axis as well as torsional deflections about the same axis.
- The stiffness of the flexible appendages in the Y-Z plane is very high and their deformations in this plane are neglected in this model.
- The first bending modes of vibration shall be taken into account to define the performances of the system by means of a mathematical model.

Figure 1 depicts the specified spacecraft according to these assumptions and its corresponding dimensions and attitude maneuvers.

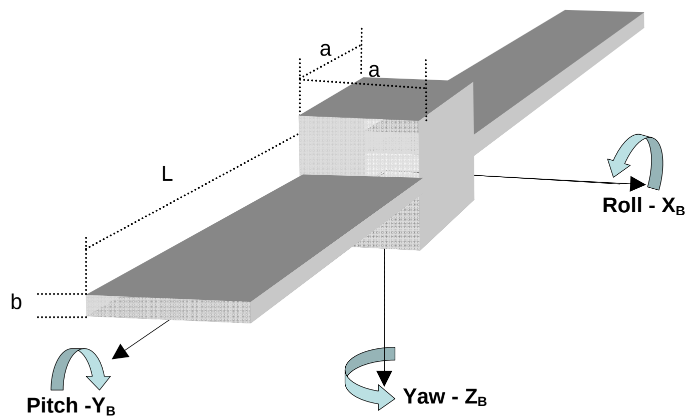

Fig. 1: Graphical representation of the spacecraft configuration.

The deformations of both solar panels are discretized by a series of admissible functions together with some associated time dependent generalized coordinates as:

$$w_i(\xi,t) = \sum_{i=1}^{2} \phi(\xi) q_i(t) \tag{1}$$

$$v(\xi, z, t) = \sum_{i=1}^{2} \psi(\xi) r_i(t)$$

The vectors $w_i(\xi, t)$ and $v(\xi, z, t)$ are the bending and torsion deformations, respectively. Here, $\phi(\xi)$ and $\psi(\xi)$ are spatial admissible functions that correspond to a clamped-free beam for the longitudinal dimension and a free-free beam for the transverse dimension. The corresponding generalized coordinates are given by $q_i(t)$ and $r_i(t)$, respectively. The index i = 1, 2 depicted in Eq. 1 corresponds to the number of solar panels specified in the spacecraft model. The solar panel deflections are measured with respect to the corresponding local body frame ($\mathbf{X_B} - \mathbf{Y_B} - \mathbf{Z_B}$). Figure 2 shows the deflections that occur around the $\mathbf{Y_B}$- and $\mathbf{Z_B}$-axis.

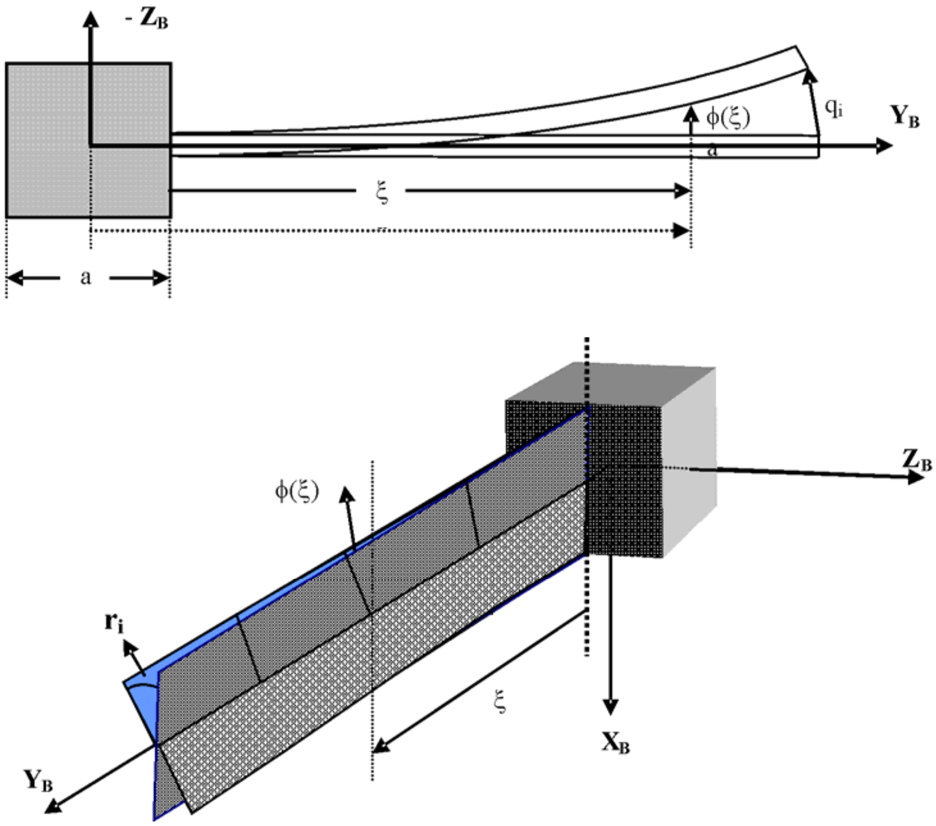

Fig. 2: Graphical representation of the flexible appendages deflections.

B. Equations of Motion

Flexible spacecraft are well described by a set of ordinary differential equations, in addition to a set of boundary conditions imposed by the system dynamics. A Lagrangian approach can often be used to formulate the nonlinear differential equations of motion. This approach is widely used to derive the differential equations that govern the motion of dynamical systems.

When applying a Lagrangian formulation, a basic step that is frequently used to obtain the equations of motion is the derivation of the system’s kinetic and potential energies. The kinetic energy includes terms that relate to spacecraft rotation and the elastic displacements of the solar panels. The potential energy includes terms that correspond to the deformations in the solar panels together with the action of the gravity gradient torque [23]. The mathematical system model is expressed in a compact form as:

$$\boldsymbol{M}\ddot{\boldsymbol{u}} + \boldsymbol{G}\dot{\boldsymbol{u}} + \boldsymbol{K}\boldsymbol{u} = \boldsymbol{Q}_{nc}\,. \qquad \textbf{(12)}$$

Here, the mass matrix is ***M***, the gyroscopic matrix is ***G***, and the stiffness matrix is ***K.*** It should be noted that solar panels have uniform and intrinsic damping that must be considered in the governing equations [24]. The governing equation of motion is expressed in matrix form as:

$$\begin{bmatrix} I_X+I_{X2}+I_{X2} & 0 & 0 & Q_{X1} & 0 & Q_{X2} & 0 \\ 0 & I_Y+I_{Y1}+I_{Y2} & 0 & 0 & Q_{Y1} & 0 & Q_{Y2} \\ 0 & 0 & I_Z & 0 & 0 & 0 & 0 \\ Q_{X1} & 0 & 0 & m_1 & 0 & 0 & 0 \\ 0 & Q_{Y1} & 0 & 0 & J_{Y1} & 0 & 0 \\ Q_{X2} & 0 & 0 & 0 & 0 & m_2 & 0 \\ 0 & Q_{Y2} & 0 & 0 & 0 & 0 & J_{Y2} \end{bmatrix} \begin{bmatrix} \ddot{\phi} \\ \ddot{\theta} \\ \ddot{\psi} \\ \ddot{q}_1 \\ \ddot{r}_1 \\ \ddot{q}_2 \\ \ddot{r}_2 \end{bmatrix} + \omega_0 \begin{bmatrix} 0 & 0 & I_Y-I_Z-I_X & 0 & 0 & 0 & 0 \\ 0 & 0 & 0 & 0 & 0 & 0 & 0 \\ I_X+I_Z-I_Y & 0 & 0 & 0 & 0 & 0 & 0 \\ 0 & 0 & 0 & \delta_1 & 0 & 0 & 0 \\ 0 & 0 & 0 & 0 & \delta_2 & 0 & 0 \\ 0 & 0 & 0 & 0 & 0 & \delta_1 & 0 \\ 0 & 0 & 0 & 0 & 0 & 0 & \delta_2 \end{bmatrix} \begin{bmatrix} \dot{\phi} \\ \dot{\theta} \\ \dot{\psi} \\ \dot{q}_1 \\ \dot{r}_1 \\ \dot{q}_2 \\ \dot{r}_2 \end{bmatrix} + \begin{bmatrix} 4\omega_0^2(I_Y-I_Z) & 0 & 0 & 0 & 0 & 0 & 0 \\ 0 & 3\omega_0^2(I_X-I_Z) & 0 & 0 & 0 & 0 & 0 \\ 0 & 0 & \omega_0^2(I_Y-I_X) & 0 & 0 & 0 & 0 \\ 0 & 0 & 0 & K_{F1} & 0 & 0 & 0 \\ 0 & 0 & 0 & 0 & K_{T1} & 0 & 0 \\ 0 & 0 & 0 & 0 & 0 & K_{F2} & 0 \\ 0 & 0 & 0 & 0 & 0 & 0 & K_{T2} \end{bmatrix} \begin{bmatrix} \phi \\ \theta \\ \psi \\ q_1 \\ r_1 \\ q_2 \\ r_2 \end{bmatrix} = \begin{bmatrix} Q_x \\ Q_Y \\ Q_z \\ 0 \\ 0 \\ 0 \\ 0 \end{bmatrix}$$

The associated generalized coordinate vector is given by $\boldsymbol{u} = \begin{bmatrix} \phi & \theta & \psi & q_1 & r_1 & q_2 & r_2 \end{bmatrix}^T$, which includes the attitude maneuvers $\begin{bmatrix} \phi & \theta & \psi \end{bmatrix}$ and solar panel deflections $\begin{bmatrix} q_1 & r_1 & q_2 & r_2 \end{bmatrix}$. The terms designated as $\dot{\boldsymbol{u}}$ and $\ddot{\boldsymbol{u}}$ are the first and second time derivatives of $\boldsymbol{u}$, respectively. This equation represents the non linear equation of motion for the spacecraft model.

The forces applied to any spacecraft depend on its orbit. In general, external perturbations consist of aerodynamic, solar pressure and magnetic forces applied to the spacecraft. Internal forces applied by spacecraft actuators, such as reaction wheels, magneto-torques, control moment gyros, and thrusters, also must be included. In this model, the external moments exerted on the spacecraft are considered negligible in comparison to the moments exerted by control moments. The generalized forces applied to the spacecraft considered herein are:

$$\boldsymbol{Q_{nc}} = \begin{bmatrix} \boldsymbol{Q}_X & \boldsymbol{Q}_Y & \boldsymbol{Q}_Z & 0_{(n-m)} \end{bmatrix}^T$$

where, $\boldsymbol{Q}_X$, $\boldsymbol{Q}_Y$ and $\boldsymbol{Q}_Z$ are the internal forces generated by internal actuators.

C. Linearization Process

The nonlinear model of a rigid-flexible spacecraft shows a large amount of coupling with their mechanical parts. In this sense, the attitude motion is coupled with the deformations of flexible appendages. Roll and yaw maneuvers are coupled, and they are also coupled with bending vibrations. Pitch attitude maneuvers are coupled with torsional deformations.

The system represented in Eq. (12) is linearized around the system equilibrium´s position, which is defined as $\phi = \theta = \psi = 0$, $q_1 = q_2 = 0$ and. $r_1 = r_2 = 0$. This linearization process allows us to express the dynamics of the system in a convenient form such that the control law can be developed as:

$$\begin{aligned} \dot{\overline{\boldsymbol{x}}} &= \boldsymbol{A}\overline{\boldsymbol{x}} + \boldsymbol{B}\overline{\boldsymbol{u}} \\ \overline{\boldsymbol{y}} &= \boldsymbol{C}\overline{\boldsymbol{x}} + \boldsymbol{D}\overline{\boldsymbol{u}} \end{aligned} \qquad \textbf{(13)}$$

where $\boldsymbol{A}$ is the state matrix, $\boldsymbol{B}$ is the control matrix, $\boldsymbol{C}$ is the output matrix, and $\boldsymbol{D}$ is the matrix that correlates inputs and controlled variables for the system.

An approach to the study of system stability is given by Eq. (12) and may be achieved using a linearized equation of motion that is close to equilibrium. The mass matrix $\boldsymbol{M}$ is considered a positive definite, the gyroscopic matrix $\boldsymbol{G}$ is a skew symmetric matrix, and the stiffness matrix $\boldsymbol{K}$ will be positive definite if the system is performing around equilibrium and is stable. The system's stability depends on the moment inertia values and the spacecraft configuration when developing its orbit.

III. Control Problem

The objectives of the control law applied to this type of vehicle may focus on several aspects. The most important of these relate to vibration control, amplitude control and the decoupling of dynamic modes when the system remains stable. These performances relate to the eigenstructure of the system. The stability of the system is obtained using appropriate system eigenvalues, such that vibration, amplitude and decoupling performances relate to the amplitude of the corresponding elements of closed loop eigenvectors. By following these requirements, an EA method may be an appropriate technique for the design of a control law that is applicable to a flexible spacecraft.

We considered the linear system (13) with n states, m inputs and p outputs, where the vector of states is $\bar{\boldsymbol{x}}$, $\bar{\boldsymbol{y}}$ is the vector of measurements and $\bar{\boldsymbol{u}}$ is the control vector. The state matrix is $\boldsymbol{A} \in \Re^{nxn}$, the control matrix is $\boldsymbol{B} \in \Re^{nxm}$, the matrix of observable states is $\boldsymbol{C} \in \Re^{pxn}$ and $\boldsymbol{D} \in \Re^{pxn}$ is the matrix that relates inputs and outputs.

The relationship of system matrices to the mass, gyroscopic and stiffness matrices is given by:

$$\boldsymbol{A} = \begin{bmatrix} 0 & \boldsymbol{I}_{nxn} \\ -\boldsymbol{M}^{-1}\boldsymbol{K} & -\boldsymbol{M}^{-1}\boldsymbol{G} \end{bmatrix} \quad \boldsymbol{B} = \begin{bmatrix} 0 \\ \boldsymbol{M}^{-1}\begin{bmatrix} 0_{(n-m)xm} \\ \boldsymbol{I}_m \end{bmatrix} \end{bmatrix} \boldsymbol{C} = [\boldsymbol{I}] \ \boldsymbol{D} = [0] \qquad \textbf{(16)}$$

where the state vector $\bar{\boldsymbol{x}}(\boldsymbol{t})$ is a function of the attitude angles (ϕ, θ, ψ), the bending of flexible appendages (q_1, r_1, q_2, r_2), and their corresponding first derivatives, which are expressed as:

$$\bar{\boldsymbol{x}}(\boldsymbol{t}) = \begin{bmatrix} \phi & \theta & \psi & q_1 & r_1 & q_2 & r_2 & \dot{\phi} & \dot{\theta} & \dot{\psi} & \dot{q}_1 & \dot{r}_1 & \dot{q}_2 & \dot{r}_2 \end{bmatrix}^T \qquad \textbf{(17)}$$

The dynamic coupling found in this type of vehicle may be a potential problem based on the assumption that one of the primary requirements for the behavior of a closed loop system is the need for an acceptable level of decoupling in the system. With this in mind, the time response of the system (13) is expressed as:

$$\boldsymbol{y}(t) = \boldsymbol{C}\sum_{i=1}^{n}\boldsymbol{v}_i e^{\lambda_i t}\boldsymbol{w}_i^T\boldsymbol{x}(0) + \sum_{i=1}^{n}\boldsymbol{v}_i\boldsymbol{w}_i^T\int_0^t \boldsymbol{C}e^{\lambda_i(t-\tau)}\boldsymbol{Bu}(\tau)d\tau \qquad \textbf{(18)}$$

where the system eigenvalues are represented by λ_i, the right eigenvector by a set of $\boldsymbol{v_i}$ and the left eigenvector by a set of $\boldsymbol{w_i^T}$. This expression depicts the relation that exists between the time response of the system and their eigenvalues, right and left eigenvectors, system inputs and initial conditions. In addition, the homogeneous component of $\boldsymbol{y}(t)$ is given by:

$$\boldsymbol{y}(t) = \boldsymbol{C}\sum_{i=1}^{n}\boldsymbol{v}_i e^{\lambda_i t}\boldsymbol{w}_i^T\boldsymbol{x}(0)$$

The interesting aspects shown in this expression are based on the mathematical modes given by $e^{\lambda_i t}\boldsymbol{w}_i^T\boldsymbol{x}(0)$ and by the system coupling expressed as $\boldsymbol{Cv}_i$. The solution to the control problem in this paper is focused on obtaining a static controller given by $\boldsymbol{K}$ (mxp). Assuming that all of the states are available, the control law is represented as:

$$\vec{\boldsymbol{u}} = -\boldsymbol{K}\vec{\boldsymbol{y}} = -\boldsymbol{KC}\vec{\boldsymbol{x}} \qquad \textbf{(19)}$$

In order to achieve closed loop stability and decouple targets for a rigid-flexible system, the general EA method establishes a set of desired eigenvalues and their associated desired eigenvectors for a closed loop system, which is known as a desired eigenstructure and is designated as Λ_d and $\boldsymbol{V}_d$ by the following elements:

$$\Lambda_d = \left[\lambda_{d1}........\lambda_{dp}\right]$$
$$\boldsymbol{V}_d = \left[v_{d1}.......v_{dp}\right]$$

With regard to the decoupling of system modes, the elements of the desired eigenvectors must be selected in such way that their values are zero. If this requirement is met, the corresponding system decoupling will be obtained. This means that the amplitude of the free end of the solar panel will be several times smaller than that of the open loop system. In addition, the interaction among rigid, bending and torsion modes will also be less.

The primary task in the development of the control law is the determination of the feedback gain matrix $\boldsymbol{K}$ such that the eigenvalues and eigenvectors of the closed loop system are as close as possible to the desired eigenstructure.

Several techniques have been developed to design suitable controllers according to a desired eigenstructure for closed loop system. In general, these techniques focus on parametric and low sensitivity eigenstructure assignments. The first method accounts for the value of the eigenvalues in order to establish the best method to solve the problem. The second method addresses the problem using recursive methods, where the primary objective is the robustness of the system. For the purpose of this paper, it is useful to consider a parametric eigenstructure. Assuming that matrix $\boldsymbol{D}=0$, the closed loop system will be given as:

$$\begin{aligned}\dot{\boldsymbol{x}} &= \left(\boldsymbol{A}+\boldsymbol{BKC}\right)\boldsymbol{x} \\ \boldsymbol{y} &= \boldsymbol{Cx}\end{aligned} \qquad \textbf{(20)}$$

The feedback problem is finding a real matrix $\boldsymbol{K}$ such that the eigenvalues of $\left(\boldsymbol{A}+\boldsymbol{BKC}\right)$ include the desired eigenvalues λ_{di} as a subset and that the eigenvectors are as close as possible to the desired eigenvectors v_{di}.

For any pair of desired closed loop eigenvalues λ_i and their associated eigenvectors v_i, Eq. (20) can be expressed as:

$$\left(\boldsymbol{A}+\boldsymbol{BKC}\right)v_i = \lambda_i v_i \qquad \textbf{(21)}$$

where the system eigenvectors are $v_i = \left(\lambda_i \boldsymbol{I}-\boldsymbol{A}\right)^{-1}\boldsymbol{BKC}v_i$. The allowable subspace is defined by the columns of the matrix $\left(\lambda_i \boldsymbol{I}-\boldsymbol{A}\right)^{-1}\boldsymbol{B}$. Then, the best achievable eigenvector may be obtained by projecting the desired eigenvector onto the allowable subspace. In Eq. (21), the state matrix for a closed loop system may be expressed as:

$$\left[\boldsymbol{A}-\lambda_i\boldsymbol{I} \quad \boldsymbol{B}\right]\begin{bmatrix} v_i \\ \boldsymbol{KC}v_i \end{bmatrix} = 0 \qquad \textbf{(22)}$$

This may be represented for a non trivial solution as a null space given by:

$$\begin{bmatrix} v_i \\ \boldsymbol{KC}v_i \end{bmatrix} \in \left\{\aleph : \left[\boldsymbol{A}-\lambda_i\boldsymbol{I} \quad \boldsymbol{B}\right]\right\} \qquad \textbf{(23)}$$

This null space is known as the achievable vector space. Thus, all achievable eigenvectors that correspond to the desired closed loop eigenvalues must fall in the subspace spanned by the columns of $\left[\boldsymbol{A}-\lambda_i\boldsymbol{I} \quad \boldsymbol{B}\right]$.

Therefore, the desired eigenvectors can be exactly achieved if they belong to this subspace and if there is a feedback matrix $\boldsymbol{K}$.

From Eq. (22), the vector is defined as:

$$\bar{\boldsymbol{w}}_i = \boldsymbol{K}\boldsymbol{C}v_i \qquad \textbf{(24)}$$

This is called the right parameter vector [22]. This vector, when is applied to all eigenvectors, is related to the computation of the controller as:

$$\boldsymbol{K} = \bar{\boldsymbol{W}}\left(\boldsymbol{C}\boldsymbol{V}\right)^{-1} \qquad \textbf{(25)}$$

A. Decoupling Criteria

Because the decoupling of system modes is the most important component in controller design, it is always necessary to establish the corresponding decoupling criteria. Both orbital and deformation modes can be decoupled in a closed-loop system. For example, the existing natural coupling that exists for roll and yaw motions and the associated longitudinal deflection of solar panels must be reduced for a closed loop system. Additionally, coupling between the torsional motions of solar panels and the pitch maneuvers of spacecraft must be considered candidate modes to be decoupled in a closed loop. According to these premises, the strategy required for a closed loop system regarding the coupling of modes is the method used in [27]. All of the required decoupling criteria are listed in Table 1, where a “0” indicates no coupling between modes and an “X” indicates that any value is valid.

$$\begin{bmatrix} Roll = \phi \\ Pitch = \theta \\ Yaw = \psi \\ Flexion = q_1 \\ Torsion = r_1 \\ \dot{\phi} \\ \dot{\theta} \\ \dot{\psi} \\ \dot{q}_1 \\ \dot{r}_1 \end{bmatrix} = \begin{bmatrix} 1 \\ \times \\ 0 \\ 0 \\ 0 \\ 0 \\ 0 \\ 0 \\ 0 \\ 0 \end{bmatrix}; \quad \begin{bmatrix} \times \\ 1 \\ \times \\ \times \\ 0 \\ 0 \\ 0 \\ 0 \\ 0 \\ 0 \end{bmatrix}; \quad ;\begin{bmatrix} 0 \\ \times \\ 1 \\ 0 \\ 0 \\ 0 \\ 0 \\ 0 \\ 0 \\ 0 \end{bmatrix}; \quad \begin{bmatrix} 0 \\ \times \\ 0 \\ 1 \\ 0 \\ 0 \\ 0 \\ 0 \\ 0 \\ 0 \end{bmatrix}; \quad \begin{bmatrix} 0 \\ 0 \\ \times \\ \times \\ 1 \\ 0 \\ 0 \\ 0 \\ 0 \\ 0 \end{bmatrix}$$

Table 1: Decoupling criteria applied on eigenvectors

Based on the eigenvalues, our strategy was based on two considerations. The first relates to stability and focuses on moving the unstable eigenvalue to the left-hand side of the complex plane. The second consideration relates to keeping the closed-loop eigenvalues as close as possible to the open-loop eigenvalues.

The values of the eigenvector elements depend on the assigned decoupling given in Table 1. According to this, the task is to determine the desired closed loop eigenvectors, estimated as:

$$\boldsymbol{V}_d = [\xi][\boldsymbol{V}_O]$$

where $[\xi]$ is a matrix composed of the terms expressed in Table 1. In this matrix, the elements with null values denote that the specific elements required for the desired eigenvectors have values close to zero in reference to the open loop eigenvector. The matrix $[\boldsymbol{V}_O]$ represents the open loop eigenvectors.

IV. Numerical Simulations and Results

This section presents the results of the numerical simulations carried out on the system. These simulations had, as their main objective, the verification of the decoupling of the system modes according to the requirements set forth in Table 1. The verification of dynamical decoupling was performed by a set of graphical time responses in relation to attitude maneuvers. Additionally, this simulation exhibited the effectiveness of the proposed algorithm along with the mathematical model of the rigid-flexible spacecraft.

To associate system performance to the controller design process using a parametric eigenstructure assignment process, we considered two different system situations. According to the procedure developed herein, the design process should begin by defining the desired eigenstructure. This eigenstructure was a set of desired eigenvalues and desired eigenvectors. The dynamical performances of the system exhibited a natural damping in some of the system modes. The design requirements may be adapted to obtain different damping coefficients for the system modes. In this sense, the controller design aims to assign different eigenvalues to bending and torsion modes.

A precise selection of the deformation eigenvalues should be made to obtain a minimal interaction with the rigid modes of the system. Some problems may arise due to the inappropriate selection of eigenvalues, which can cause errors in the spacecraft's attitude. To illustrate the design procedure and show some numerical results, the state matrix $\boldsymbol{A}$ and control matrix $\boldsymbol{B}$ are given as [28]:

$$
\boldsymbol{A} = \begin{bmatrix}
0 & 0 & 0 & 0 & 0 & 1 & 0 & 0 & 0 & 0 \\
0 & 0 & 0 & 0 & 0 & 0 & 1 & 0 & 0 & 0 \\
0 & 0 & 0 & 0 & 0 & 0 & 0 & 1 & 0 & 0 \\
0 & 0 & 0 & 0 & 0 & 0 & 0 & 0 & 1 & 0 \\
0 & 0 & 0 & 0 & 0 & 0 & 0 & 0 & 0 & 1 \\
8.4225\times10^{-4} & 0 & 0 & 11.012 & 0 & 0 & 0 & 3.6485\times10^{-5} & 0 & 0 \\
0 & -1.0503\times10^{-3} & 0 & 0 & 4.3090 & 0 & 0 & 0 & 0 & 0 \\
0 & 0 & -1.2383\times10^{-3} & 0 & 0 & 1.1909 & 0 & -1.2396\times10^{-3} & 0 & 0 \\
-7.9086\times10^{-4} & 0 & 0 & -7.6983\times10^{2} & 0 & 0 & 0 & -3.4259\times10^{-5} & 0 & 0 \\
0 & 1.0503\times10^{-6} & 0 & -1.6\times10^{5} & 0 & 0 & 0 & 0 & 0 & 0
\end{bmatrix}
$$

$$
\boldsymbol{B} = \begin{bmatrix}
0 & 0 & 0 \\
0 & 0 & 0 \\
0 & 0 & 0 \\
0 & 0 & 0 \\
0 & 0 & 0 \\
2.25058\times10^{-2} & 0 & 0 \\
0 & 2.6931\times10^{-2} & 0 \\
0 & 0 & 3.096\times10^{-2} \\
-2.3529\times10^{-2} & 0 & 0 \\
0 & 0 & 0
\end{bmatrix}
$$

A. Modal Analysis

This process began via an assessment of the open loop system to understand its modal system behavior. The performance of the open loop system is summarized in Table 2. The basic modal analysis was designed to investigate the effects of system modes characterized by their eigenvalues over the complete system.

As indicated in Table 2, the system modes were grouped into orbital or rigid and deformation modes. This classification demonstrated the rigid-flexible performance for this type of vehicle. The roll maneuver exhibited instability with high damping, the yaw eigenvalues exhibited poor damping, and the pitch mode performed with no damping. Two flexible modes were considered, namely, the bending and torsion modes. These modes presented a null damping at frequencies of 27.7 and 400 rad/s, respectively. The behavior of these eigenvalues was oscillatory if they were excited by attitude maneuvers. An interesting idea introduced in [29] relates to the performance of the proposed method when applied to rigid-flexible spacecraft. This is measured by identifying the modes that can be controlled and those that are uncontrolled. In addition, this approximation of the problem may be applied to the determination and attenuation of linearized undesired coupling in these vehicles.

Dynamics		Eigenvalues	Damping	Natural Frequency (rad/sec)
Orbital Modes	Roll	$\pm 2.91 \times 10^{-2}$	1.00	2.91×10^{-2}
	Pitch	$0 \pm 3.24 \times 10^{-2} i$	0.0	3.24×10^{-2}
	Yaw	$-6.15 \times 10^{-4} \pm 3.48 \times 10^{-2} i$	1.76e-002	3.48×10^{-2}
Deformation Modes	Bending	$0 \pm 27.7i$	0.0	2.77×10^{-1}
	Torsion	$0 \pm 400i$	0.0	4.00×10^{2}

Table 2: Performance of the open loop system.

The data depicted in Table 2 demonstrate that the system motion is unstable and has oscillatory deformation modes. Independent of the desired eigenvalues and eigenvectors required to calculate the controller design, the effect of deformation mode dampening is an interesting problem.

First, the problem of eigenstructure assignment and its effect on desired eigenvectors is introduced in Table 1 (“Decoupling criteria”). Second, the controller design may focus on classical requirements that relate to basic system performance, such as damping, settling time and wide band. By linking these requirements with the damping of the deformation modes, it should be possible to calculate the coupling level with attitude motions. In addition, by applying the EA method, the controller may need to satisfy multiple design criteria, including stability, performance, decoupling and robustness [30 - 31].

The EA process fits with the specified classical requirements of the pole placement part of the method, such as damping, natural frequency and time settings. In this sense, the system should first be established, followed by a second action that should focus on modifying the damping of the orbital modes. The second action is especially important. If it were possible to modify the real part of the deformation eigenvalues with only minor consequences for the rest of the modes, an acceptable system coupling would be obtained.

The depicted eigenvalue data for an open loop system indicate that the deformation modes are strictly oscillatory. This situation demonstrates that any attitude maneuver performed by the spacecraft might excite the frequencies that correspond to bending and torsion modes. The design requirement selected for the torsion mode intended to maintain the same close loop eigenvalue as that of the open loop system. Therefore, the desired eigenvalue for the first torsion frequency was equal to the open loop eigenvalue.

Thus, no additional damping or any other time performance was needed for the torsion mode in a closed loop. This decision was made based on the remote possibility that torsion frequency was not easily excited due to its value.

The possibilities that the bending eigenvalue offers are different. The first frequency bending mode can be excited by roll and yaw attitude motions. This mode of performance implies at least two operational requirements for the bending eigenvalue. The first requirement is that the desired eigenvalue for the bending mode be the same value as that of an open loop. The second possibility is related to giving additional damping to the first bending mode by means of a set of desired eigenvalues. These two design strategies represent the nominal damping (Case I) and the forced damping (Case II) scenarios in this paper.

To complete the EA design process, the desired closed loop eigenvectors are required. The system requirements presented in Table 1 are related to the values of certain eigenvectors in terms of decoupling. In this sense, a null or very attenuated coupling of the interactions of roll and yaw motions and their associated bending deformations are required. The pitch maneuver must also be decoupled from torsional deformations. These requirements indicate that the associated elements of the eigenvectors should be close to zero. A zero value for any element of the eigenvectors in a closed loop system indicates that a full decoupling has been obtained.

In the design process, by means of any of the EA methods, it is necessary to take into account the position of the obtained eigenvalues. The proximities of the obtained eigenvalues and eigenvectors to their desired values essentially depend on the algorithm and method used in the process. It is necessary to perform several trial and error tests and compare the resulting eigenstructure to the desired one

Finally, the simulations performed for Cases I and II were based on attitude maneuvers. The roll and yaw maneuvers were analyzed by considering a bending deformation, whereas the pitch channel was analyzed by considering the torsion deformation of solar panels.

B. Case I: Nominal Damping

In this section, we discuss the case in which the positions of the eigenvalues associated with bending and torsional deflections remain in the same position as those for the open loop system. The solution to this problem focuses on the acquisition of the related coupling for motions around the primary Euler axis and the associated deflections of the solar panels.

The primary purpose of this case is to characterize the system to maintain the values of the flexion and torsion eigenvalues in a closed loop such that they equal the values that have been obtained for the open loop. The values of the bending and torsion eigenvalues are located on the imaginary axis of the complex plane. This does not introduce any problems for the behavior of the entire system because the amplitude of the mentioned eigenvalues is very small; however, it is interesting to understand the actual behavior of solar panel bending for different motions around the Euler axis.

As illustrated in Table 3, the obtained eigenvalues are the same as the desired values with the exception of the pitch eigenvalue. According to these data, the roll and pitch behavior of the system in a closed loop were more dampened than that observed for the same modes in an open loop. In this case, the time response of these maneuvers was slower in comparison to the time response for the open loop system; however, the solar panel could not withstand strong bending. The pitch channel had the greatest damping in the eigenstructure assignation process. This implies that the obtained eigenvalues were different from the desired eigenvalues, but the results may be acceptable because the first torsion frequency was not easily excited. The obtained bending and torsion eigenvalues were the same as the desired values. In this case, the required deformation eigenvalues were the same as the open loop system eigenvalues.

Dynamic Modes	Desired Eigenvalues	Obtained Eigenvalues	Damping	Natural Frequency (rad/sec)
Roll	$-6.14 \times 10^{-2} \pm 3.48 \times 10^{-2}i$	$-6.15 \times 10^{-2} \pm 3.48 \times 10^{-2}i$	8.70×10^{-1}	7.06×10^{-2}
Pitch	$-8.67 \times 10^{-2} \pm 3.24 \times 10^{-2}i$	-1.40×10^{-2} -1.60×10^{-2}	1.00	1.40×10^{-2} 1.60×10^{-1}
Yaw	$-2.9 \times 10^{-2} \pm 2.9 \times 10^{-2}i$	$-2.90 \times 10^{-2} \pm 2.90 \times 10^{-2}i$	9.95×10^{-2}	2.91×10^{-1}
Flexion	$-0.00 \pm 2.7 \times 10^{1}i$	$0.00 \pm 2.7 \times 10^{1}i$	0.00	2.70×10^{1}
Torsion	$-0.00 \pm 4.0 \times 10^{2}i$	$0.00 \pm 4.00 \times 10^{2}i$	0.00	4.00×10^{2}

Table 3: Case I: Performance of the system in a closed loop.

Figure 4 graphically depicts the time response of the system according to the design criteria when a roll maneuver is performed. The attitude maneuver showed a light coupling for the roll and yaw channels, which induced a permanent, low amplitude vibration on the solar panel. This vibration could be considered a mathematical response due to its amplitude; however, this vibration could also be a mechanical response that represents a real situation. It is interesting to note that according to Fig. 4, a precise decoupling between the roll and yaw motions was not obtained. This means that an error in the yaw channel will persist for the permanent time response.

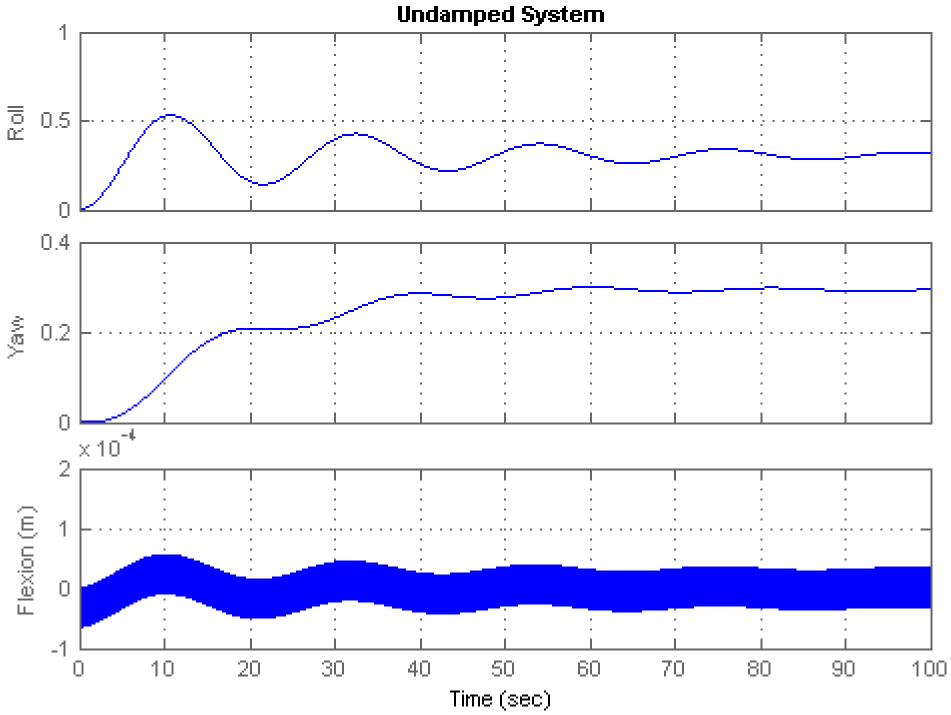

Fig. 3: Effects of roll maneuver on the yaw axis and solar panel bending.

C. Case II: Forced Damping

Based on the results obtained for Case I, this section presents the results obtained when the bending eigenvalues were modified via the introduction of additional damping. This additional damping was obtained by the requirements specified in the controller design, and it must be understood as a forced damping. According to data depicted in Table 3 and the graphs depicted in Fig. 3, the bending eigenvalue was nominally coupled with the roll and yaw channels. The purpose of this study was to add damping to the bending mode to obtain a decoupled response.

By applying the design method using an EA process, some of the design eigenvalues may be affected, which could result in an eigenstructure that is different from the desired outcome. The purpose of a complete process is to obtain a specific damping for the deformation modes that is different from natural damping by applying an eigenstructure assignment.

This process checked the behavior of the system by moving the aforementioned eigenvalues to more damping positions in the complex plane. Several trial and error process were evaluated and special attention was taken to find the desired eigenvalues for the rest of the modes.

As a result of these tests, we decided to maintain the torsion eigenvalue in the same position as that of the open loop system. Moving this eigenvalue to a damper position could cause undesirable eigenvalues for the rest of the modes. Given the configuration of the spacecraft, this scenario must be acceptable because the possibility of exciting the mentioned mode is relatively small due to its frequency. Referring to the desired eigenvectors, this situation is the same as that of the nominal damping case depicted in Table 1.

As indicated in Table 4, the desired and obtained eigenvalues were practically the same. We found that the roll, pitch and yaw eigenvalues remained at the same positions in the complex plane as was observed in Case I. The design strategy also retained the same value for the torsion mode. The difference between the two cases was the bending mode. In Case II, the design process required an additional damping of 7%. The expected relationship between damping and bending deflection is indicated in Fig. 6.

Dynamic Modes	Desired Eigenvalues	Obtained Eigenvalues	Damping	Natural Frequency (rad/sec)
Roll	$-6.14 \times 10^{-2} \pm 3.48 \times 10^{-2}i$	$-6.15 \times 10^{-2} \pm 3.48 \times 10^{-2}i$	8.70×10^{-1}	7.06×10^{-2}
Pitch	$-8.67 \times 10^{-2} \pm 3.24 \times 10^{-2}i$	-1.40×10^{-2} -1.60×10^{-2}	1.00	1.40×10^{-2} 1.60×10^{-1}
Yaw	$-2.9 \times 10^{-2} \pm 2.9 \times 10^{-2}i$	$-2.90 \times 10^{-2} \pm 2.90 \times 10^{-2}i$	9.95×10^{-2}	2.91×10^{-1}
Flexion	$-20 \pm 2.7 \times 10^{1}i$	$20 \pm 2.7 \times 10^{1}i$	5.95×10^{-1}	3.36×10^{1}
Torsion	$-0.00 \pm 4.0 \times 10^{2}i$	$-4 \times 10^{-3} \pm 4.00 \times 10^{2}i$	0.00	4×10^{2}

Table 4: Case II: Performance of the system in a closed loop.

Figure 4 depicts the time response to a step input on the roll channel. The responses of the roll, yaw and bending mode depict a light coupling of the roll channel with the yaw axe. This is similar to what was observed in Case I and must be considered relatively important due to the spacecraft's configuration. The solar panel bending displayed a significantly different behavior. The maintained vibration was canceled and the amplitude of the deflections was zero. As expected, the addition of damping to the bending mode caused a minor vibration in the solar panel.

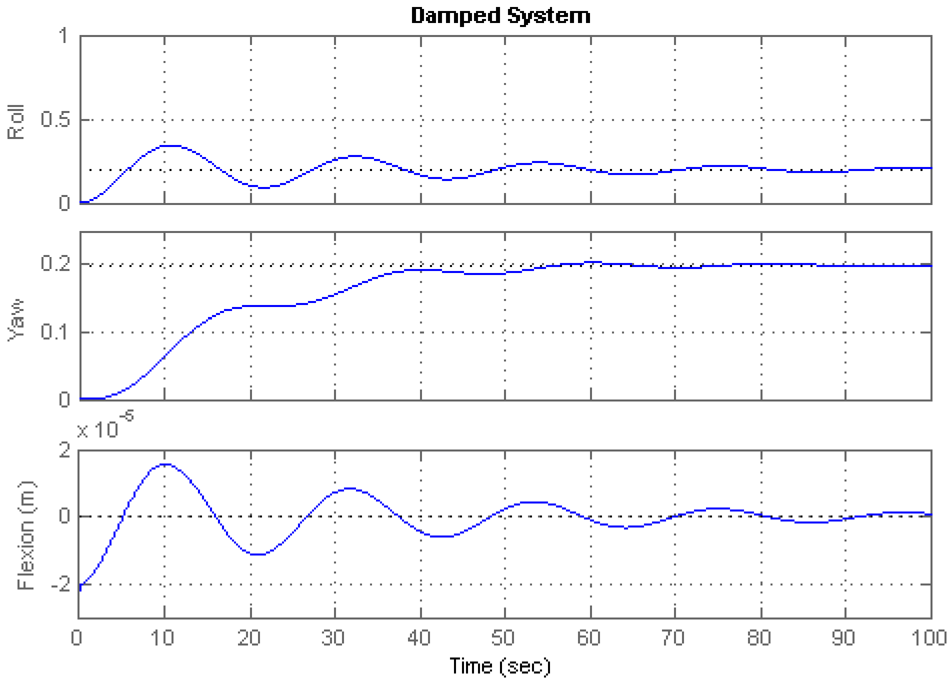

Fig. 4: Effects of the roll maneuver on the yaw axis and solar panel bending.

A second test was performed to understand the system's behavior when the spacecraft performs a yaw maneuver. A commanded step input was performed on the yaw axis to understand its influence on the roll attitude channel and the bending of the solar panels. The results depicted in Fig. 5 indicate that the coupling between the roll channel and the amplitude of the solar panel deflections was zero.

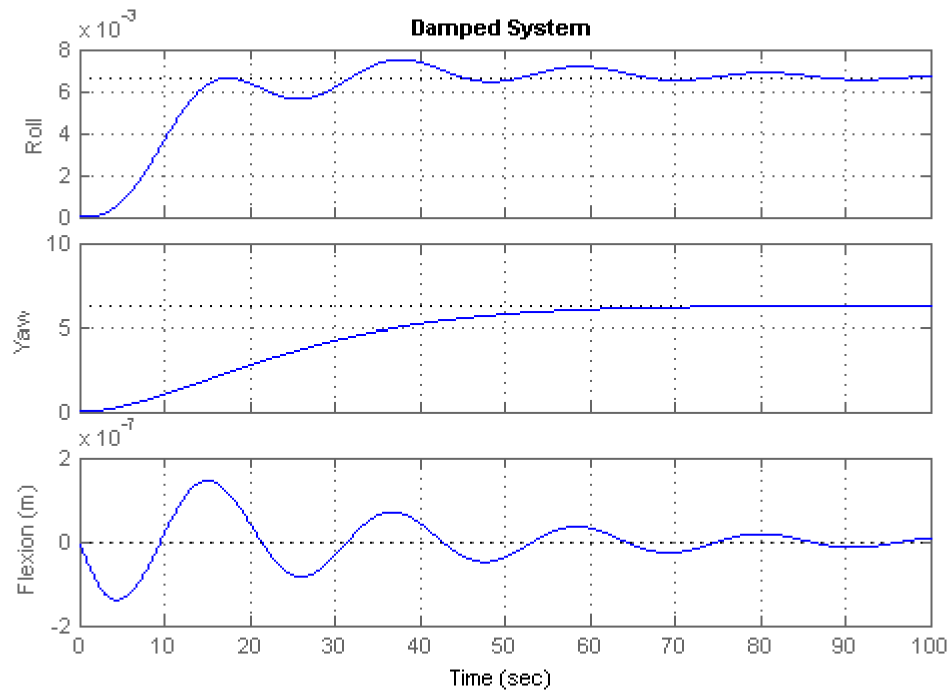

Fig. 5: Effects of a yaw maneuver on the roll axis and solar panel bending.

The tests performed on the system of Case II depicted in Fig. 4 and Fig. 5 were based on the expected results depicted in Fig. 6. The addition of damping to the bending mode caused a progressive reduction of the deflections of the solar panels. The design process must take into account the influence of the damping factor on the rest of system modes.

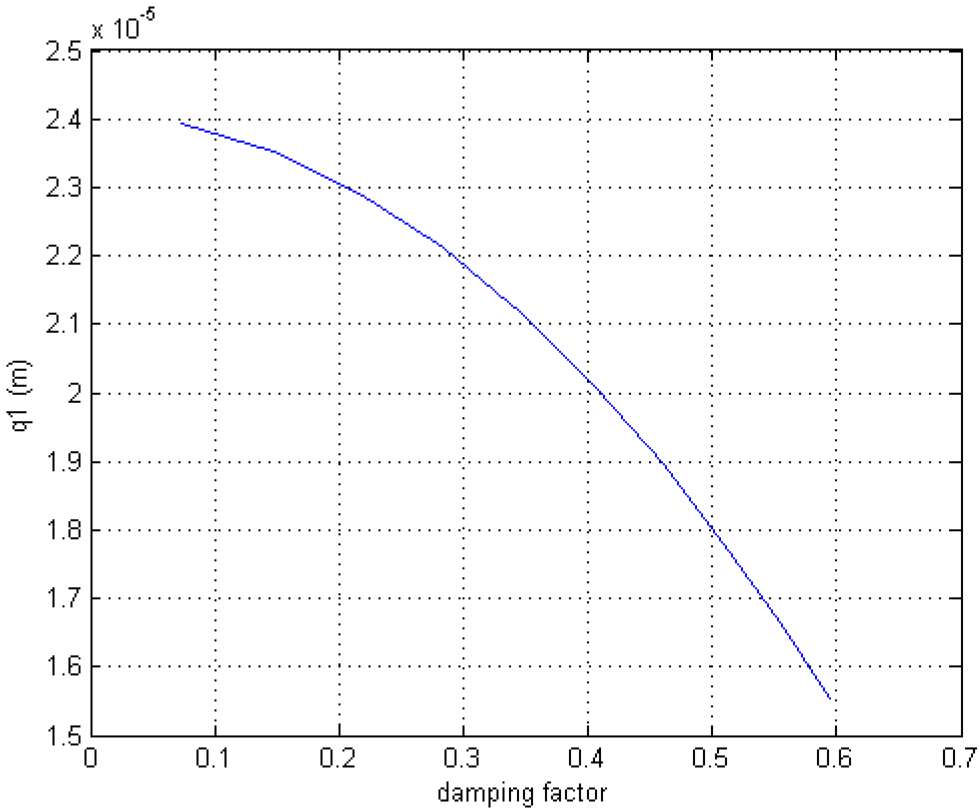

Fig. 6: Evolution of solar panel bending as a function of the damping factor.

By comparing the graphical results of Fig. 4 and Fig. 5, it is possible to conclude that any motion around the yaw axis causes a lighter induced motion around the roll axis and that the bending deformation was smaller in the second case. Although the roll and pitch maneuvers were coupled, the second had a lesser effect on system attitude and solar panel deformation. These results are consistent with the desired eigenstructure, particularly with the desired eigenvectors.

D. Torsion

Because torsional deformation is related to pitch attitude maneuvering, the requirement set on Table 1 was required to obtain the maximum decoupling degree for these two modes. Figure 6 depicts the graphical results that relate the pitch motion to the torsional deformation of the solar panels. By comparing the time response to the step command on the pitch channel, we observed that a high damping was obtained for the orbital and deformation modes with a null amplitude. It is difficult to excite the torsion mode via a pitch maneuver due to its frequency value.

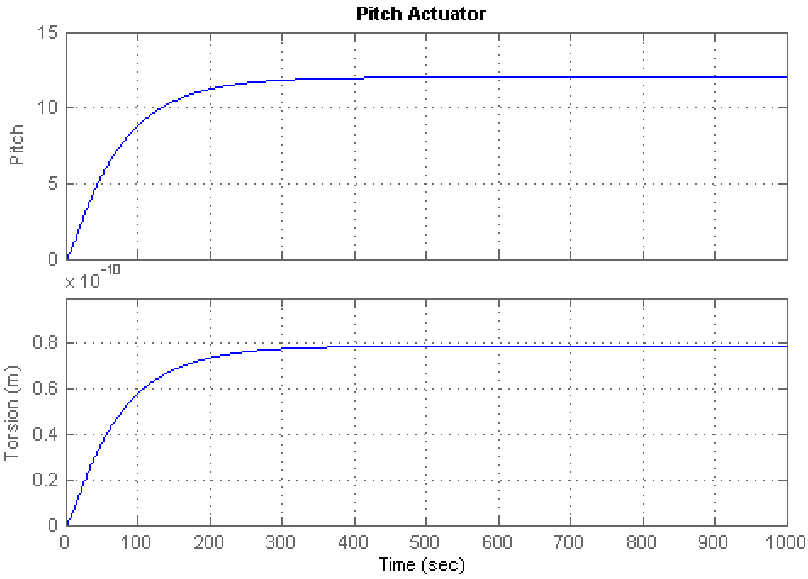

Fig. 7: Effect of pitch maneuvering on solar panel torsional deformation.

E. Robustness Analysis

Robustness analysis is carried out to evaluate the performance of the controller due to modeling and parameter uncertainties. The object of these simulations is assesses the robustness of the closed loop system with the EA controller. This analysis allows us to determine those critical performance frequencies. The robustness of the closed loop system is investigated in respect to both stability and performance measures. High frequency unmodeled dynamics and closed loop stability are related with stability robustness while performance robustness is related with acceptable system performance like settiling time and overshoot.

Any change in the dynamics or internal parameters of the spacecraft may represent a lack of robustness. It is also necessary to consider the action of non-modelled dynamics and its uncertainty on the parameters of the system. All of these factors affect the robustness and tolerance of the system to both internal and external disturbances.

The method used to asses the robustness of the system is based on the structured singular value - μ and concretely in the μ-analysis. By means of the μ-analysis will be analyzed the robust stability and the robust performance of the system when is considered as an uncertain model.

Also, linear fractional transformation (LFT) has been used to model the system with the aforementioned disturbances. Figure 8 shows the LFT model in which Δ represents the system uncertainty, $\boldsymbol{K}$ is the EA controller and finally $\boldsymbol{M}$ is the set of spacecraft model and controller.

This LFT model is the right candidate to perform a μ-analysis. μ-analysis methods are used to determine the system robustness with structured and unstructured uncertainty. The structured singular value μ, is defined as the inverse of the smallest destabilizing perturbation of a transfer function matrix and is defined as:

$$\mu(M) = \frac{1}{\min_{\Delta \in \mathbf{\Delta}} \{\bar{\sigma}(\Delta) : \Delta \in \mathbf{\Delta} \det(I - \Delta M) = 0\}}$$

Where $\bar{\sigma}(\Delta)$ denotes the maximum singular value. Therefore, $\mu(M)$ is a measure of the smallest value of Δ that causes instability of the system.

The data provided by the μ-analysis are the upper and lower bounds for the μ values over a defined frequency domain. This analysis will be performed for the candidate controller ***K***. The upper and lower bounds do not allow an accurate approximation of the structured singular value $\mu(M)$. This implies that conclusions about robust stability and robust performance need to be taken from the evolution of the μ bounds. From the analysis point of view, the robust performance goal for any frequency is $\mu(M(j\omega)) < 1$.

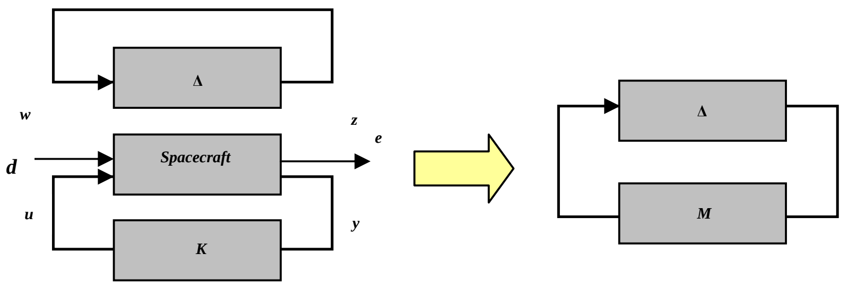

Figure 8: Linear fractional model.

In the LFT representation Δ describes the structured perturbations matrix that in the most general frame is expressed as:

$$\Delta := \left\{ \left[\Delta = diag\left[\delta_1 I_{r_1}, ..., \delta_s I_{r_S}, \Delta_1, ..., \Delta_f \right] \right] : \delta_i \in C, \Delta_j \in C^{m_j x m_j} \right\}$$

The structured singular value according to the graphical LFT represented in Figure 6 must be taken as a stability margin with respect to the structured uncertainty block affecting ***M*** being expressed as:

$$\mu_\Delta(M(s)) := \sup_{\omega \in \Re} \mu_\Delta(M(j\omega))$$

Where δ_i are the known system uncertainties. Once the uncertainty structure has been represented, the problem is focused on compute a frequency response of ***M*** and computes the structured singular value μ with respect to the uncertainty block Δ.

The robust stability and robust performance are obtained by weighting functions, which allow the estimation of the upper and lower bounds for all frequencies in the system. Figure 7 depicts the system behaviour with respect to robustness performance and robustness stability. Both response behaviours perform below the critical value of one, which demonstrates that the system shows robust performance for all of the frequencies considered. The frequency response corresponding to the robust stability shows a peak close to one located around the flexion frequency. This response is appropriate for the nature of the system, and the frequency belongs to the first vibration mode (flexion mode).
Figure 9 also shows that the calculated lower bounds for robust performance and robust stability can not be determined accurately for some frequencies. This means that performing the μ-analysis none uncertainty has been obtained to unstabilize the system. Mathematically speaking this result is related

with the real uncertainty block used in the block-structure of the uncertainty. Therefore, there is no $\varDelta \in \Delta$ such that $\det\left(I - \varDelta M\right) = 0$. In this case the structured singular value is $\mu_{\Delta}\left(M\left(s\right)\right) = 0$.

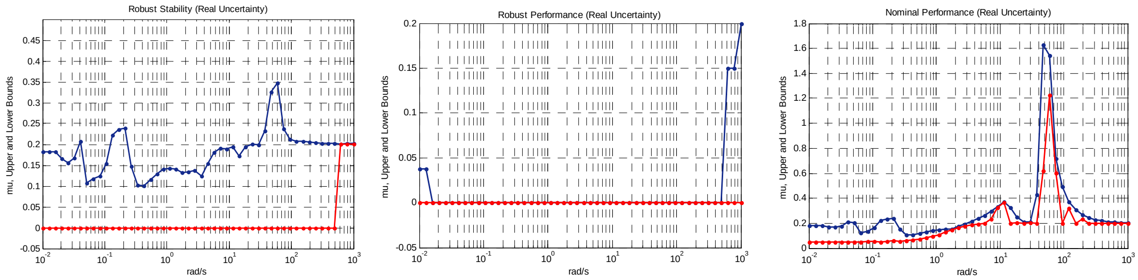

Figure 8: Results from the mu- analysis.

V. Conclusions

In this paper, we presented a method to compensate for and minimize the bending effects of solar panels during attitude maneuvers in a rigid-flexible spacecraft. We considered that the rigid-flexible spacecraft could be subjected to orbital and vibrational solar panel disturbances. The spacecraft was mathematically modeled to be a vehicle with rigid and flexible parts. This approach to the equations of motion allowed us to establish mechanical system behavior that describes the interactions of the rigid parts of the spacecraft and the flexible elements attached to them. This approach was developed to investigate the problem of the reorientation of a spacecraft with flexible appendages. Several technical challenges are associated with the study of an ill-conditioned system due to the values of elements within the state matrix $\boldsymbol{A}$. This implies a poor original system robustness that must be accounted for during the controller design process. One of the primary problems with this type of vehicle is the extent of coupling between the rigid and flexible elements of the structure. Spacecraft performance was obtained by means of a modal analysis to detect the frequencies of interest together with their magnitude, damping and coupling with other frequencies. The static controller was designed by taking into account two different cases in which the damping was the parameter of interest. The results of the analyzed cases show that the EA controllers agree with the required eigenstructure. We have shown that it is possible to obtain an acceptable decoupling for some system modes. Additional damping was also added to the bending mode by means of a second EA controller. The torsion mode was found to be excited only by pitch maneuvers, and furthermore, this mode was difficult to excite due to its frequency. Nevertheless, in this study, we were able to specify those requirements related with mechanical coupling.

References

[1] Meirovitch, L. and Quinn, R. D: “Equations of motion for maneuvering flexible spacecraft”. Journal of Guidance, Vol 10, no. 5, Sept – Oct 1987.

[2] Meirovitch, L. and Stemple, T: “Hybrid equations of motion for flexible multibody systems using quasicoordinates”. Journal of Guidance, Control and Dynamics, Vol 18, no. 4, July-August 1995.

[3] Di Gennaro, S: “Active vibration suppression in flexible spacecraft attitude tracking”. Journal of Guidance, Control and Dynamics, Vol. 21, no. 3, May – June 1998.

[4] Quinglei Hu:”Input shaping and variable structure control for simultaneous precision positioning and vibration reduction compensation”. Journal of Sound and Vibration 318 (2008), pp.18 – 35.

doi: 10.1016/j.jsv.2008.03.068

[5] Ishimura, K. and Higuchi, K: “Coupling between structural deformation and attitude motion of large planar space structures suspended by multi-tethers”. Acta Astronautica 60 (2007), pp. 691 – 710.

doi: 10.1016/j.actaastro.2006.10.002

[6] Cai, G.P. and Lim, C. W:”Dynamics studies of a flexible hub-beam system with significant damping effect”. Journal of Sound and Vibration 318 (2008), pp. 1 – 17.

doi: 10.1016/j.jsv.2008.06.009

[7] Maganti, G. B. and Singh, S. N: ”Simplifies adaptive control of an orbiting flexible spacecraft”. Acta Astronautica 61 (2007), pp. 575 – 589.

doi: 10.1016/j.actaastro.2007.02.004

[8] Fonseca, I. M., Bainum, P. M., Silva, A. R: “Structural control interaction for an LSS attitude control system using thrusters and reaction wheels”. Acta Astronautica 60 (2007), pp. 865 – 872.

doi: 10.1016/j.actaastro.2006.11.008

[9] Komatsu, K., Kida, T et al: “On orbit system identification and attitude control experiment of ETS-VI”. Electronic version. Cited 15, April, 1997.

[10] Wonham, W. M: “On pole assignment in multi-input controllable linear systems”. NASA Technical report, 67-2, February, 1967.

[11] Moore, B. C.: “On the flexibility offered by state feedback in multivariable systems beyond closed loop eigenvalue assignment” Short Paper, IEEE Transactions on automatic control, October 1976, pp. 689-692.

[12] Kimura, H: “Pole assignment by gain output feedback”. IEEE Transactions on automatic control, August 1975, pp. 509-516.

[13] Andry,A.N, Shapiro, E.Y. and Chung, J. C.” Eigenstructure Assignment for Linear Systems. IEEE Transactions On Aerospace And Electronic Systems Vol. AES-19, no. 5 September 1983, pp. 711-729.

[14] J. M. de la Cruz, Ruipérez, J, Aranda, J: “RCAM design challenge presentation document: an Eigenstructure Assignment Approach”. Group for Aeronautical Research and Technology in Europe, GARTEUR, TP-088-22, April 1997.

[15] Faleiro, L. F., Magni, J. F., De la Cruz, J. M., Scala, S.: “Robust Flight Control”, Cap. 3. ISBN 978-3-540-76151-8, pp. 22-32.

[16] Juang, J, Lim, K. and Junkins, J. L: “Robust eigensystem assignment for flexible structures”. Journal of Guidance, Vol 12. no. 3, May – June 1989, pp. 381-387.

[17] Nieto-Wire, C., Sobel, K. “Eigenstructure Assignment for a Tailless Aircraft”. AIAA paper 2007-6417, Aug. 2007.

[18] Kron, J., de Lafontaine, J and Daniel Alazard. “Robust 2-DOF H-infinity Controller for Highly Flexible Aircraft: Design Methodology and Numerical Results”. Canadian Aeronautics and Space Journal. Vol. 49, no 1, March 2003, pp. 19-29.

[19] Oliva, A. P., Leite Filho, W. C.”Eigenstructure versus Optimal Control for Decoupling”. Control Engineering Practice, 2002, pp. 1059-1079.

[20] Faleiro, L. and Pratt, R. “RCAM Design Challenge Presentation Document: An Eigenstructure Assignment Approach”, GARTEUR/TP-088-18, April 1997.

[21] Magni, J.F. ”Robust Modal Control with a Toolbox for Use with MATLAB”, ONERA-Toulouse. Kluwer Academic/Plenum Publishers, 2002. ISBN 0-306-46773-9.

[22] Liu, P. and Patton, R.J., “Eigenstructure Assignment Toolbox for Use with MATLAB”, Pacilantic International Ltd. Oxford. 1999. ISBN 0953389014.

[23] Meirovich, L. “Methods of Analytical Dynamics”, McGraw-Hill, Inc, 1970, pp. 72-85. ISBN: 0-07-041455-6.

[24] Maybeck, Peter S.; Schore, Michael R.“Reduced Order Multiple Model Adaptive Controller for Flexible Spacestructure”. IEEE Transaction on Aerospace and Electronic Systems, Vol. 28, nº 3, July 1992.

[25] Leissa, A. W: ”Vibration in Plates”.NASA SP-160, 1969.

[26] Sarafin, T. P:”Spacecraft structures and mechanisms – From Concept to Lunch”. Kluwer Academic Publishers, 1995, pp. 184-188. ISBN: 0-7923-3476-0.

[27] Aranda, J., Crespo, J. “Modal Analysis Applied to Spacecraft Attitude Control”. AIAA paper 2007-6444, Aug. 2007.

[28] Crespo, J., Aranda, J. “Eigenstructure assignment-based controllers applied to flexible spacecraft”. Proc. IMechE Vol. 225 Part G; Journal of Aerospace Engineering. DOI: 10.1177/2041302510393027.

[29] Jae Weon Choi. “Spillover Supression via Eigenstructure Assignment in Large Flexible Structures”. Journal of Guidance, Vol. 25, 2002. Engineering Notes.

[30] Bruyere, L, Tsourdos, A and B. A. White. “Quasilinear Parameter-Varying Autopilot Design Using Polynomial Eigenstructure Assignment with Actuator Constraints”. Journal of Guidance, Control and Dynamics. Vol. 29, No. 6, November–December 2006.

[31] Kron, J. de Lafontaine, LePeuvédic, C. “Mars Entry and Aerocapture Robust Control Using Static Output Feedback and LPV Techniques”, Proceedings of the 6th International Guidance Conference on Guidance, Navigation and Control Systems, October 2005, ESA SP-606 Loutraki, Greece.